

## Fast decoherence of slowly relaxing polarons in semiconductor InAs quantum dots

F. BRAS<sup>1</sup>, S. SAUVAGE<sup>1</sup>, G. FISHMAN<sup>1</sup>, P. BOUCAUD<sup>1(\*)</sup>,  
J.-M. ORTEGA<sup>2</sup> and J.-M. GÉRARD<sup>3</sup>

<sup>1</sup> *Institut d'Électronique Fondamentale, UMR CNRS 8622, Bâtiment 220  
Université Paris-Sud - 91405 Orsay, France*

<sup>2</sup> *CLIO-Lure, Bâtiment 209 D, Université Paris Sud - 91405 Orsay, France*

<sup>3</sup> *CEA-Grenoble, DRFMC-PSC - 38054 Grenoble Cedex 9, France*

received 11 February 2005; accepted in final form 21 March 2005

published online 8 April 2005

PACS. 78.67.Hc – Quantum dots.

PACS. 78.47.+p – Time-resolved optical spectroscopies and other ultrafast optical measurements in condensed matter.

PACS. 71.38.-k – Polarons and electron-phonon interactions.

**Abstract.** – We report on polaron dynamic measurements in InAs/GaAs semiconductor quantum dots. The polaron dynamics is monitored by transient nonlinear spectroscopy by recording the transmission variation as a function of the pulse area of an infrared picosecond excitation. A non-monotonous transmission is observed for pulse areas larger than a  $\pi$  pulse. We attribute this transmission dependence with pulse area to a signature of damped optical Rabi oscillation of polarons. The damping of the Rabi oscillation is modeled by two level optical Bloch equations. A short dephasing time  $T_2$  around 5 ps is deduced for the resonantly excited polaron, one order of magnitude smaller than the relaxation time. We show that the decoherence of the polaron state is not limited by its slow relaxation but rather by the fast dephasing of its phonon component.

The coherent control of quantum states is a key mechanism for quantum information processing and manipulation of quantum bits (qubits). One typical example of coherent nonlinear light-matter interaction are the optical Rabi oscillations between discrete levels [1]. In a two-level system driven by a strong resonant optical field, the Rabi oscillations correspond to the temporal evolution of the population difference between the discrete states. The population oscillates between the upper and lower states at a frequency proportional to the dipole matrix element of the optical transition and the electric field amplitude of the driving excitation. The Rabi oscillations can be evidenced by time-integrated measurements as a function of the input pulse area.

In semiconductors, the short dephasing times associated with charge excitations require the use of ultrashort optical pulses with a femtosecond or picosecond duration to coherently drive the system. Direct observation of optical Rabi oscillations have been first reported in

---

(\*) E-mail: philippe.boucaud@ief.u-psud.fr

quantum wells using a two-color pump probe scheme resonant with excitonic excitations [2]. More recently, considerable efforts have been devoted to study coherent phenomena in semiconductor quantum dots. Semiconductor quantum dots are potential candidates as building blocks for quantum information processing. The dephasing times associated with interband optical excitations in quantum dots are longer than in quantum wells, thus facilitating the observation of coherent interactions [3]. Optical Rabi oscillations have been observed for resonant interband excitations in individual self-assembled quantum dots [4, 5] or in quantum dots naturally formed at quantum well interfaces [6] as well as in the excitonic ground-state transition of an InGaAs quantum dot ensemble [7].

In semiconductor quantum dots, the confined states cannot be treated near the phonon resonances as simple discrete pure electronic states of an artificial atom. Coherent phonon processes associated with the nearly dispersionless optical phonons have to be considered. A strong-coupling regime occurs for the carrier-phonon interaction leading to the formation of quasiparticles called polarons [8]. The polarons are mixed entangled electron-phonon eigenstates accounting for the electron - optical phonon interaction through the Fröhlich Hamiltonian, *i.e.* the polarons correspond to linear combinations of unperturbed states which diagonalize the Fröhlich Hamiltonian. The existence of polarons has drastic consequences on the quantum dot energy spectra [9, 10] as well as on the carrier dynamics and relaxation in quantum dots [11–13]. While it was shown that the polaron formalism is adequate to understand the carrier dynamics between discrete states probed by intersublevel excitation [14], no experimental study has been carried out to illustrate the effect of polaron formation on coherent optical excitation in quantum dots. Moreover, the dephasing properties of the coherently excited polaron has not been addressed so far.

In this work, we report on the coherent dynamics of InAs/GaAs quantum dot polarons as measured by transient nonlinear optical spectroscopy. The quantum dot polarons are coherently excited with picosecond infrared optical pulses delivered by a free-electron laser. The population flopping is monitored by probing the population inversion in a non-colinear pump-probe configuration scheme. The transmission decrease observed for large pulse areas is interpreted as a signature of optical Rabi oscillations. The damping of the oscillation provides an estimate of the dephasing time  $T_2$  of the polaron of  $\sim 5$  ps. The dephasing time is much shorter than the relaxation time  $T_1$ , but of the same order of magnitude than the dephasing time of the coherently excited optical phonon.

The investigated sample was grown by molecular beam epitaxy. It consists of 30 *n*-doped InAs quantum dot layers separated by 50 nm thick GaAs barrier layers. The dot density is  $4 \times 10^{10} \text{ cm}^{-2}$ . At low temperature, an average occupation number of 1.2 electron in the dots was measured by intersublevel absorption [15]. Around 20  $\mu\text{m}$  wavelength, the polaron absorption is split along two orthogonal polarization directions, namely  $[-110]$  and  $[110]$ . The coherent dynamics of the polarons was driven with the picosecond optical pulses delivered by the free-electron laser CLIO (Centre Laser Infrarouge d'Orsay). The laser is tuned in resonance with the polaron absorption polarized along the  $[110]$  direction. A normalization procedure as described in ref. [14] based on a ratio between successive macropulses delivered by the free-electron laser was used in order to enhance the signal-to-noise ratio. The experiments were performed at low temperature in an helium flow cryostat with the sample set at normal incidence.

Figure 1 shows the spectral dependence of the polaron absorption measured with the free-electron laser as compared to a continuous wave measurement. When the pump and probe pulses are coincident in time, the pump pulse induces a partial bleaching of the polaron absorption and an increase of the transmission of the probe. The amplitude of the polaron absorption is measured from this probe variation transmission. The probe pulse average power was 2 orders of magnitude smaller than the pump pulse. The polaron absorption is

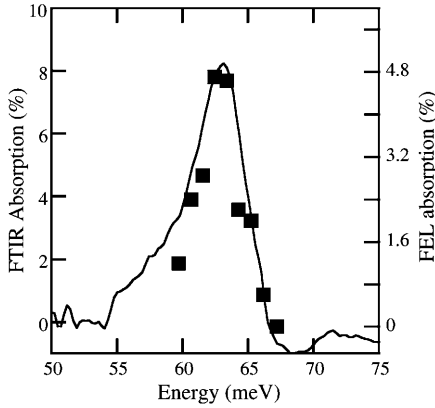


Fig. 1

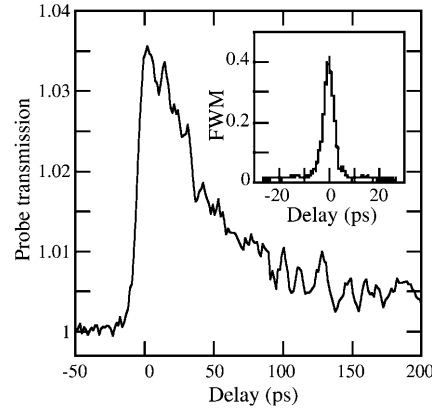


Fig. 2

Fig. 1 – Low-temperature (5 K) polaron absorption measured with a Fourier-transform infrared spectrometer (full line, left scale) or by differential transmission in pump-probe measurement at zero time delay with a free-electron laser (squares, right scale).

Fig. 2 – Probe transmission as a function of time delay between pump and probe. The resonant excitation of the polaron is set at 62 meV. The temperature is 5 K. The inset shows the third-order autocorrelation spectrum of the picosecond exciting pulse.

resonant around 63 meV with a 5 meV full width at half-maximum. Three-dimensional 8 band  $\mathbf{k} \cdot \mathbf{p}$  calculation of the quantum dot electronic structure [16] taking into account the small correction of the energies due to the electron-phonon coupling [17] indicates that this energy is consistent with a lens-shaped InAs dot with lateral sizes of 25 nm along [110], 28 nm along  $[-110]$  and an height of 2.5 nm. The broadening of the absorption corresponds to an in-plane size variation of  $\pm 5\%$ , *i.e.* a dipole variation of  $\pm 5\%$ . This transition dipole variation does not account for the fluctuation resulting from shape variation and composition of the islands. At the energy of 63 meV, the weight of the 1-phonon component in the polaron eigenstate is around 5% [17]. Figure 1 shows that the absorption as measured with the free-electron laser closely follows the continuous wave measurement. The difference in absorption amplitude is attributed to an incomplete bleaching of the polaron absorption by the pump pulse. In the following, the dynamic experiments were performed for a resonant excitation at 62 meV (19.9  $\mu\text{m}$  wavelength).

Figure 2 shows a low-temperature pump-probe measurement for a resonant excitation at 62 meV. A monoexponential decay of the polaron is observed with a  $T_1$  characteristic time of 45 ps. A previous study has shown that the polaron decay is driven by the instability of its phonon part [14]. This instability, which results in a finite longitudinal optical (LO) phonon lifetime, is triggered by three phonon mechanisms and the decay of zone center longitudinal optical phonons as a consequence of the anharmonicity of the lattice forces [11]. The  $T_1$  value measured at the energy of 62 meV is lower than the values reported previously at lower energy [14]. We emphasize that at this energy, the polaron state can no longer be discussed in terms of zero- and one-phonon components alone. The polaron level is significantly closer to the two-phonon resonance and the weight of the two-phonon component in the polaron state is expected to be non-negligible ( $\sim 1$  percent). An intermediate polaron state at lower energy corresponding to the orthogonal direction is also present. The direct correlation with polaron decay data reported in ref. [14] is thus not straightforward. We have observed that

the  $T_1$  value deduced from the pump-probe measurement remains constant at low excitation density and increases at high excitation densities with a relaxation dynamics deviating from a monoexponential decay. This effect is likely associated with the coupling of polarons and the transfer of the excitation through the phonon [18]. The inset of fig. 2 shows a degenerate four-wave mixing measurement of the incoming pulse resulting from the interaction with the third-order nonlinear susceptibility of the substrate. This measurement provides the third-order autocorrelation function of the incident pulses [19]. The full width at half-maximum of the four-wave mixing autocorrelation signal is around 5 ps, corresponding to an incoming pulse with  $\sim 4$  ps full width at half-maximum duration assuming a Gaussian temporal pulse shape.

Figure 3 shows the amplitude variation of the probe at zero time delay as a function of the incident pump pulse area. Similar results and curve shapes were obtained for different positive time delays [6]. The pulse area was varied by inserting grid attenuators in the optical path. The duration of the pulses was kept constant. At a given delay, the amplitude of the probe transmission is proportional to the population difference between the ground and excited polaron states. As seen in fig. 3, the amplitude of the probe transmission is controlled by the pump strength. The probe transmission first increases as a function of the pulse area and exhibits an oscillation with a clear decrease after the first maximum. A minimum is observed for a pulse area about two times larger than the pulse area corresponding to the first maximum, followed by a slight increase at larger pulse areas. We attribute this non-monotonous dependence to a signature of optical Rabi oscillations, *i.e.* a signature that the polaron state is coherently driven by the optical field. We rule out thermal effects as the origin of the transmission variation because of the weak average power density incident on the sample. In an ideal homogeneously broadened two-level system, the population inversion exhibits an oscillatory behavior driven by the pulse area  $\Theta$  and proportional to  $\sin^2[\Theta/2]$  with  $\Theta = \frac{\mu}{\hbar} \int_{-\infty}^{+\infty} E(t) dt$ , where  $\mu$  is the dipole matrix element,  $\hbar$  the reduced Planck constant and  $E$  the amplitude of the electric field. In time-integrated experiments, this time evolution corresponds to an oscillatory behavior as a function of the integrated pulse area with maxima for a succession of odd  $\pi$  pulses and minima for even  $\pi$  pulses. In view of the experimental uncertainties on the pulse parameters for a  $20 \mu\text{m}$  excitation wavelength (spot size, profile, homogeneity, etc.), the experimental value of the pulse area at first maximum is compatible with a  $\pi$  pulse. The differential transmission measurement reported in fig. 3 shows a strong damping of the oscillation. As shown below, this damping is a direct consequence of the existence of the electron-phonon quasiparticle. This damping was numerically modeled by solving the optical Bloch equations for an ensemble of two-level systems [1]. The differential transmission is calculated by integrating over the inhomogeneous broadening of the transition. The model accounts for the inhomogeneous broadening resulting from the transition dipole variation and for the finite pulse duration as deduced from the third-order autocorrelation. The inhomogeneous spatial profile of the incident pulse is also taken into account. This spatial inhomogeneity leads to an additional damping of the oscillations as the wings of the pulse do not contribute to the population inversion like the center of the pulse. Additionally, the spatial inhomogeneity leads to a contraction of the Rabi oscillations. The model does not account for the renormalization of Rabi oscillations assisted by phonon interaction [20]. Because of the picosecond time scale of the experiment, we do not consider the coherent non-equilibrium lattice displacements of LO phonons which are expected to occur on a much shorter time scale ( $\sim 110$  fs for 36 meV phonons) as well as lattice relaxation processes and non-adiabatic effects [21–23].

Figure 4(a) shows the calculated population inversion variation,  $-(\Delta n_{\text{pump}} - \Delta n_0)/\Delta n_0$  where  $\Delta n_{\text{pump}}$  and  $\Delta n_0$  are the population inversion with or without the pump, respectively, for a  $T_2$  lifetime of 5 ps as a function of a Gaussian distribution of dipole moments. The dipole variation given in percent corresponds to the standard deviation  $\sigma$  of a Gaussian distribution.

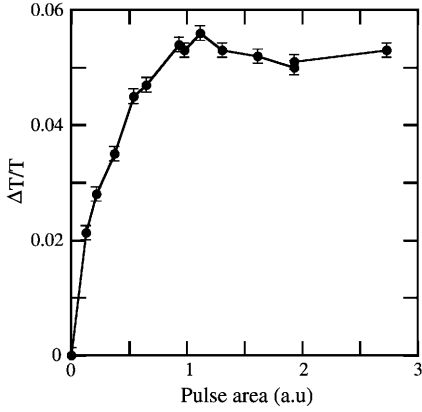


Fig. 3

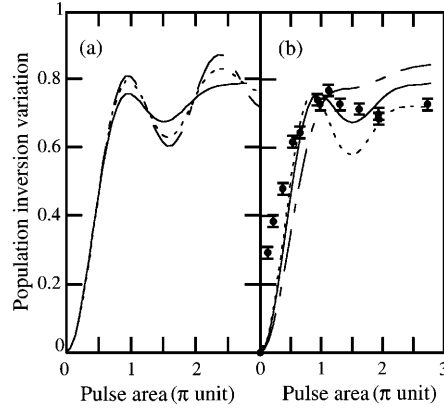


Fig. 4

Fig. 3 – Differential transmission variation of the polaron as a function of the incident pulse area. The transmission variation is measured at zero time delay between pump and probe. The dots correspond to experimental measurements with a polaron excitation at 62 meV. The full line is a guide to the eye.

Fig. 4 – (a) Population inversion variation for a  $T_2$  dephasing time of 5 ps for different distribution of dipole moments (standard deviation). Dashed line: no dispersion; dotted line: 10% dipole fluctuation; full line: 20% dipole fluctuation. (b) Population inversion variation for a dipole dispersion of 20% and different  $T_2$  dephasing times. Dashed line:  $T_2 = 2$  ps; full line:  $T_2 = 5$  ps; dotted line:  $T_2 = 10$  ps. The experimental data points (full dots) as shown in fig. 3 are superimposed on the simulation lines, their amplitude being normalized by the continuous wave absorption amplitude.

As expected, the damping is more pronounced as the broadening of the dipole distribution increases. The main source of the damping stems from the ensemble effect. In the following, we have considered a standard deviation of 20% for the dipole fluctuation, a value larger than the value deduced by the dot size fluctuation for a fixed aspect ratio of the dots. This value accounts for dipole fluctuation induced by shape and composition fluctuation of the islands. A similar strong dipole fluctuation was phenomenologically introduced to model Rabi oscillations in the excitonic ground-state transition of InGaAs quantum dots [7]. Figure 4(b) shows the effect of the dephasing time value on the damping of the oscillations for a fixed inhomogeneous broadening. The damping related to the contrast of the first oscillation becomes more pronounced as the dephasing time decreases and gets closer to the pulse duration. We can deduce an estimate of the dephasing time from the damping and contrast of the oscillation. As the damping depends, for a fixed pulse duration, on the dephasing time and on the inhomogeneous dipole fluctuation, the accuracy on the dephasing time is limited by the choice of the dipole distribution, as well as by the approximation of a two-level system. The couple  $\{T_2, \sigma\}$  of relevant parameters is determined by maximizing the agreement with the experimental data, in particular to get as close as possible to the observed contrast of the oscillation (first maximum *vs.* first minimum) and to the absorption amplitude for the highest intensity data points. A satisfying agreement is obtained for a dipole variation with a standard deviation of 20% and a  $T_2$  time of 5 ps. This set of parameters corresponds to the full line of fig. 4(b) and is compared with the experimental data points as shown in fig. 3, normalized by the continuous wave absorption amplitude. It is clear from fig. 4(b) that the strong damping of the oscillation contrast can only be accounted for a value of  $T_2$  around 5 ps, a value estimated by assuming a significant dipole variation with  $\sigma = 20\%$ , *i.e.* an inhomogeneous

distribution already leading to a strong damping (fig. 4(a)). A larger (smaller) value of  $T_2$ , such as those considered in fig. 4(b), would lead to a stronger (vanishing) oscillation contrast respectively, not experimentally observed. A larger value of  $\sigma$  would not be realistic, in view of the inhomogeneous distribution of the dots and does not lead to a satisfactory agreement with the data as is also the case for a smaller value of  $\sigma$  along with a shorter value of  $T_2$ . The 5 ps value of  $T_2$  is thus estimated with an uncertainty error of less than a factor of 2. Note that the measured normalized amplitude of the first maximum (0.77) can be obtained from the ratio between the transmission variation at 62 meV as measured in fig. 3 (5.6%) and the transmission variation as measured in fig. 1 (7.2%). A very good agreement is obtained with the calculated value (0.77). A deviation is observed between measurements and calculation for weak pulse areas. This deviation is attributed to the uncertainty on the pulse area value for weak excitation since the insertion of successive grid attenuators can modify the intensity by changing the beam focalization. Note that the development of a more sophisticated model with the introduction of additional intermediate states as recently proposed in the case excitonic Rabi oscillation [24] could improve the agreement between experimental and theoretical curves, but is beyond the scope of this letter.

The 5 ps value of the dephasing time is significantly shorter than the standard value expected from the  $T_2 = 2T_1$  (*i.e.* 90 ps) relation if the polaron dephasing is supposed limited by relaxation processes. In the case of bulk materials, coherent time-resolved investigation of LO phonon dynamics in GaAs has shown that the phonon dephasing is governed by the phonon lifetime. This feature was determined by time-resolved coherent anti-Stokes Raman scattering as reported in ref. [25], where the relation  $T_2 = 2T_1$  was shown to be valid for the phonon dephasing. The modeling of the Rabi oscillations as reported in fig. 4 indicates that the dephasing time of the polaron is close to the pulse duration and thus much shorter than the polaron relaxation time. The polaron is a quasiparticle with a phonon component which has a short lifetime ( $\sim 5$  ps at low temperature by reference to the measurements on bulk GaAs phonons, *i.e.* not accounting for the phonon confinement and the InAs composition of the dots) and a dephasing time governed by its relaxation. The decoherence of the polaron will thus occur on the time scale of the phonon lifetime as the polaron is entangled with the environment after a characteristic time given by the dephasing of its phonon component. The dephasing of the polaron is thus not dependent on the weight of the 1-phonon component in the quasiparticle even if the polaron relaxation time depends on the weight of the 1-phonon component. In other words, the coherent electron-phonon exchange resulting from the strong-coupling regime and observed in the relaxation of the polaron vanishes on the time scale of the phonon relaxation time, while the polaron relaxation occurs on a much longer time scale for a large detuning from the anticrossing [11]. Our experiments thus confirm experimentally that the dephasing time of the polaron is of the order of the dephasing time of its phonon component without considering its weight in the quasiparticle. It also confirms that the formation of the polarons and the instability of the phonons are crucial to understand the dynamics and the coherence properties in the dots.

This result can be compared with those obtained in other strongly coupled systems such as polaritons. In the case of polaritons, by analogy with atomic microcavity physics, the linewidth of the polariton resonances  $\gamma_{\text{pol}}$  at zero detuning corresponding to the anticrossing is given by  $\gamma_{\text{pol}} = (\gamma_{\text{exc}} + \gamma_{\text{cav}})/2$ , where  $\gamma_{\text{exc}}$  is the exciton linewidth and  $\gamma_{\text{cav}}$  is the cavity linewidth associated with the photon lifetime [26]. Direct time-domain observation of polariton Rabi oscillations indicate that the oscillations decay with a characteristic time  $1/\gamma_{\text{pol}}$ , independently of the detuning [27]. In the case of the polaron, the linewidth of the electronic excitation is negligible if one considers that the very slow spontaneous emission of photons is the only dephasing path for the electron. The damping of Rabi oscillations is thus given by  $2/\gamma_{\text{phonon}}$  with

$\gamma_{\text{phonon}} = 1/T_1$  where  $T_1$  is the phonon lifetime but not the polaron lifetime. The decoherence of the polaron is two times larger than the  $T_2$  time of the coherently excited phonon.

In conclusion, we have performed transient nonlinear optical spectroscopy in resonance with InAs/GaAs quantum dot polaron transition. A non-monotonous differential transmission was observed as a function of the pulse area, a dependence attributed to a signature of optical Rabi oscillation. The dephasing time  $T_2 \sim 5$  ps for the resonantly excited polaron is much shorter than the polaron relaxation time and of the same order of magnitude than the dephasing time of the coherently excited bulk phonon. We have shown that the dephasing of the polaron is not given by the dephasing of its phonon part balanced by its weight in the quasiparticle, *i.e.* is not limited by relaxation, but is rather given by the dephasing of its phonon component.

## REFERENCES

- [1] ALLEN L. and EBERLY J. H., *Optical Resonance and Two-Level Atoms* (Wiley, New York) 1975.
- [2] SCHÜLZGEN A. *et al.*, *Phys. Rev. Lett.*, **82** (1999) 2346.
- [3] BORRI P. *et al.*, *Phys. Rev. Lett.*, **87** (2001) 157401.
- [4] KAMADA H. *et al.*, *Phys. Rev. Lett.*, **87** (2001) 246401.
- [5] HTOON H. *et al.*, *Phys. Rev. Lett.*, **88** (2002) 87401.
- [6] STIEVATER T. H. *et al.*, *Phys. Rev. Lett.*, **87** (2001) 133603.
- [7] BORRI P. *et al.*, *Phys. Rev. B*, **66** (2002) 81306(R).
- [8] INOSHITA T. and SAKAKI H., *Phys. Rev. B*, **56** (1997) R4355.
- [9] FOMIN V. M. *et al.*, *Phys. Rev. B*, **57** (1998) 2415.
- [10] HAMEAU S. *et al.*, *Phys. Rev. Lett.*, **83** (1999) 4152.
- [11] LI X.-Q., NAKAYAMA H. and ARAKAWA Y., *Phys. Rev. B*, **59** (1999) 5069.
- [12] VERZELEN O., FERREIRA R. and BASTARD G., *Phys. Rev. B*, **62** (2000) R4809.
- [13] VERZELEN O., FERREIRA R. and BASTARD G., *Phys. Rev. B*, **64** (2001) 75315.
- [14] SAUVAGE S. *et al.*, *Phys. Rev. Lett.*, **88** (2002) 177402.
- [15] BRAS F. *et al.*, *Appl. Phys. Lett.*, **80** (2002) 4620.
- [16] BOUCAUD P. and SAUVAGE S., *C. R. Phys. (Paris)*, **4** (2003) 1133.
- [17] HAMEAU S. *et al.*, *Phys. Rev. B*, **65** (2002) 85316.
- [18] WOGGON U. *et al.*, *Phys. Rev. B*, **67** (2003) 45204.
- [19] SCHULZ H., SCHÜLER H., ENGERS T. and VON DER LINDE D., *IEEE J. Quantum Electron.*, **25** (1989) 2580.
- [20] FÖRSTNER J., WEBER C., DANCKWERTS J. and KNORR A., *Phys. Rev. Lett.*, **91** (2003) 127401.
- [21] STEINBACH D. *et al.*, *Phys. Rev. B*, **60** (1999) 12079.
- [22] JACAK L., MACHNIKOWSKI P., KRASNYJ J. and ZOLLER P., *Eur. Phys. J. D*, **22** (2003) 319.
- [23] VAGOV A., AXT V. M. and KUHN T., *Phys. Rev. B*, **66** (2002) 165312.
- [24] VILLAS-BÔAS J. M., ULLOA S. E. and GOVOROV A. O., *Phys. Rev. Lett.*, **94** (2005) 57404.
- [25] VALLÉE F. and BOGANI F., *Phys. Rev. B*, **43** (1991) 12049.
- [26] CARMICHAEL H. J. *et al.*, *Phys. Rev. A*, **40** (1989) 5516.
- [27] JACOBSON J. *et al.*, *Phys. Rev. A*, **51** (1995) 2542.